Lab on a Chip

Microscope-based light gradient generation for quantitative growth studies of photosynthetic micro-organisms

Journal:	*Lab on a Chip*
Manuscript ID	LC-ART-04-2022-000393.R1
Article Type:	Paper
Date Submitted by the Author:	26-May-2022
Complete List of Authors:	Liu, Fangchen; Cornell University, Department of Biological and Environmental Engineering Gaul, Larissa; Cornell University, Department of Biological and Environmental Engineering Shu, Fang; Cornell University, Department of Biological and Environmental Engineering Vitenson, Daniel; Cornell University, Department of Biological and Environmental Engineering Wu, Mingming; Cornell University, Department of Biological and Environmental Engineering

ARTICLE

Microscope-based light gradient generation for quantitative growth studies of photosynthetic micro-organisms

Received 00th January 20xx,
Accepted 00th January 20xx

DOI: 10.1039/x0xx00000x

Fangchen Liu, † Larissa Gaul, † Fang Shu, Daniel Vitenson and Mingming Wu *

Photosynthetic micro-organisms are equipped with molecular machineries that are designed to transform light into chemical or bioenergy, and help shape and balance the ecosystem of all life forms on earth. Recently, aquatic ecosystems have been disrupted by climate change, which leads to the frequent occurrence of harmful algal blooms (HABs). HABs endanger drinking water resources and harm the fishing and coastal recreation industries. Despite its urgency, mechanistic understanding of how key biophysical and biochemical parameters impact algal growth is largely unexplored. In this article, we developed a microscope-based light gradient generator for studies of photosynthetic micro-organisms under well-defined light intensity gradients. This technology utilized a commercially available microscope, allowed for controlled light exposure and imaging of cells on the same microscope platform, and can be integrated with any micrometer scale device. Using this technology, we studied roles of light intensity in the growth of photosynthetic micro-organisms. A parallel study was also carried out using a 96 well plate. Our work revealed that the growth rate of the microalgae/cyanobacteria was significantly regulated by the light intensity and followed Monod or van Oorschot kinetic models. The measured half-saturation constants were compared with those obtained in macroscale devices, and indicated that shading, light spectrum, and temperature may all play important roles in the light sensitivity of photosynthetic micro-organisms. This work highlighted the importance of analytical tools for quantitative understanding of biophysical parameters in the growth of photosynthetic micro-organisms and knowledge learned will be critical in the future designs of technologies for managing algal blooms as well as optimizing bioenergy production.

Introduction

A quantitative understanding of photosynthetic micro-organisms (PSMs) is important for developing a sustainable future that includes both clean energy and a clean environment. Cyanobacteria, a main group of PSMs, were the first living cells that evolved the ability to harness light energy and transform it into chemical and bioenergy/biomass, and were believed to eventually enable the presence of complex life forms on earth [1, 2]. The growth of PSMs is closely controlled by light, in addition to many environmental factors, including nutrients and temperature. Understanding how PSMs interact with environmental factors allows us to design solutions that maintain the balance of ecological systems and develop alternative energy sources.

An emerging environmental problem today is harmful algal blooms (HABs), that disrupt the aquatic ecosystem balances. The occurrence of HABs is increasing due to climate change and population growth [3-6]. HABs are a sudden growth of harmful algae in both fresh and saltwater. Many HAB-forming species can produce toxins that further deteriorate water resources. Various environmental cues, including nutrients, temperature, light, and fluid flow, have been found to influence the occurrence of HABs [7-12]. Light is a key factor controlling photosynthesis and thus the bloom biomass accumulation. Specifically, light conditions have been found to affect the competition between the toxigenic and nontoxigenic strains of *Microcystis aeruginosa (M. aeruginosa)*, a widespread freshwater bloom-forming cyanobacteria [13-15]. Therefore, the ability to predict, control, and prevent HABs requires systematic investigation into the behavior of HAB-forming species under controlled light conditions.

An equally pressing problem we face today is the increase of greenhouse gas in the earth's atmosphere due to the excessive use of fossil fuels. Using PSMs to transform solar energy into biofuel provides a promising avenue for alternative energy. Microalgae and cyanobacteria are competitive candidates for bioenergy production, an alternative to fossil fuels, due to their fast growth rate, high oil content per acre, and ability to be cultured in photo-bioreactors [16-18]. In addition to biofuels including bioethanol, biodiesel, biohydrogen, and biogas [19], other high-value products have been produced from microalgae and cyanobacteria cultures successfully [20]. The ability of microalgae and cyanobacteria to grow in eutrophic water and wastewater also makes them useful in bioremediation, where removal of unwanted substance can be coupled with valuable

Department of Biological and Environmental Engineering, Cornell University, Ithaca, NY, USA.E-mail: mw272@cornell.edu.
† These authors contributed equally.
Electronic Supplementary Information (ESI) available: [details of any supplementary information available should be included here]. See DOI: 10.1039/x0xx00000x

production [21, 22]. Moreover, Algae-Microbial Fuel Cell (A-MFC), which uses algae culture in the cathode chamber of a microbial fuel cell (MFC), enables bioelectricity production along with biomass production, biorefinery, and bioremediation [23, 24]. The quality and efficiency of algal bioenergy production, bioremediation, and product creation critically depends on light conditions.

Both macro- and micro- scale technologies have been developed for a basic understanding of how PSMs interact with light. The impact of light intensity on the growth of *M. aeruginosa,* a major contributor to freshwater HABs, has been studied using batch or continuous culture under the illumination of fluorescent or LED lamps. It was found that both photoperiodicity and irradiance regulate photosynthesis, and the high intraspecies variation (or heterogeneity) among *M. aeruginosa* cells enabled them to better survive the extreme low or high light conditions [25-27]. We note that the macro-scale culture methods often experience the self-shading effect and are not suitable for mechanistic understanding of cellular response to light. Recently, researchers have developed methods to precisely control the intensity, spectrum, and spatial distribution of light at micro-scale, combined with microfluidics, to follow light-dependent cell growth in both space and time, screen microalgal oil production, or study the light-sensitive cell motility [28-36]. Graham et al. developed an array of miniaturized photobioreactor for the screening of light properties such as intensity and spectral composition on photosynthetic growth [29]. In this system, the light intensity of each individual well was directly controlled by the programmable Liquid Crystal Display (LCD) pattern overlaid above an LED light source. However, real-time cell imaging was difficult, which limited the time-resolution of cell growth and production studies. Kim et al. studied the effect of light intensity and light-dark cycle on growth and oil production of a colonial microalgae using a multilayer microfluidic device, where a gradient of black dyes generated from mixing channels was used to control light intensities, and pneumatic microvalves were used to control light-dark cycles [36]. In addition to photosynthetic growth, some motile microalgae have phototactic behavior that is also of interest [30-34]. Lam et al. built a customized system that enabled the real-time manipulation of the swarming behavior of phototactic microalgae [35]. A digital light processing (DLP) projector and a 4x lens were used to generate light patterns with 20μm resolution onto a microfluidic chip, and live cell motion was monitored by a camera. Despite the precise spatiotemporal control, considerable amounts of instrumentation and programming effort were required.

We present the development of a microscope-based system with well-controlled light intensity gradients at micrometer scale, for high-throughput examination of the behavior of PSMs in response to light. The unique contribution of our system is the ease with which one can generate the light gradients, and the ability to control light intensity and image the PSMs within the same microscope system. This platform took advantage of the two different light paths in a commercial microscope: the transmitted light path for light gradient generation with an added light pattern mask, and the fluorescence light path for real-time imaging of the PSM cells. This technology, coupled with microfluidic platforms, can be easily expanded to provide multi-environmental parameter control besides light, such as chemical gradients and temperature. Using this platform, we studied the growth of a model microalga, *Chlamydomonas reinhardtii (C. reinhardtii)*, under Photosynthetically Active Radiance (PAR) ($\mu mol \cdot m^{-2} \cdot s^{-1}$) gradients. Results were compared against light gradient growth experiments conducted in 96-well plates. We also studied the growth of an environmentally relevant species, *M. aeruginosa*, in 96-well plates.

Materials and Methods

Micro-scale light intensity gradient generation, validation and microfluidic setup

Micrometer scale light gradient generation. The micrometer-scale light intensity gradient was generated by modifying the existing bright field illumination light path of an inverted microscope (Olympus IX81, Center Valley, CA). The bright field illumination lamp, a Halogen Lamp (Olympus U-LH100L-3), was used as the light source. During the experiment, the light-dark transition region was positioned at the middle of the illuminated field via adjusting a homemade half-moon mask in the plane perpendicular to the illumination beam.

The light intensity gradient was quantified by correlating grayscale values in a bright field image of the gradient to measurements of a PAR (Photosynthetically Active Radiation) meter (Apogee MQ-501). To do this, we used uniform illumination from the bright field illumination lamp and swept through a range of bright field lamp voltages from 1.6 V to 4.1 V with a 0.1 V step. At each voltage level, 3-5 bright field images were taken with a 4X objective and an EMCCD camera (ImagEM X2 EM-CCD camera, Hamamatsu Photonics K.K.), as well as a PAR measurement. Here, the voltage control of the light source and image taking were controlled using the cellSens imaging software (Olympus Life Science). Depending on the light intensity, images were taken with no filter, or 1 ND8 filter, or 2 ND8 filters in the transmitted light path. Exposure time of the imaging varied from 1.5 to 800 ms to ensure imaging within the dynamic range of the camera. Blanks were taken by turning off the lamp and taking an image with a 4x objective and the camera. Number of filters and exposure time were not found to affect the blank grayscale value. No ND8 filters were used when taking measurements with the PAR meter. ImageJ was used to analyze grayscale images. Fig. S1A and S1B show the adjusted mean grayscale values and measured PAR values versus lamp voltages.

Array microhabitat device fabrication, assembly and experimental setup. An agarose gel-based array microhabitat device

developed previously was used (37) in conjunction with the micro-scale light gradient setup. Briefly, a two-layer SU-8 negative photoresist photolithography was used to fabricate the silicon master with the designed patterns, one layer for microhabitats and the other for side channels. A standard soft lithography method was used to transfer the pattern to a 1mm thick agarose gel membrane. The membrane was patterned with 2 functional units. Each unit has an array of 8 x 8 microhabitats flanked by two sets of side channels. Each habitat is 100 μm × 100 μm × 100 μm in size, and each channel is 400 μm wide and 200 μm deep.

To assemble the device, first, a total of 200μL of *C. reinhardtii* cells ($7.6*10^5$cells/mL) were introduced to the top of the patterned agarose membrane. Second, the membrane, surrounded by a 1mm thick plastic spacer, was carefully sandwiched between a Plexiglass manifold and a 1 inch × 3 inch glass slide. Last, the Plexiglass manifold was screwed down to a stainless-steel frame to ensure good sealing between the microhabitats, side channels and the glass slide.

Constant perfusion of fresh medium was maintained in the side channels at a flow rate of 0.7 μL/min controlled by a syringe pump (KDS230, KD Scientific, Holliston, MA) and two 10 mL syringes (Exelint International Co., Redondo Beach, CA) filled with cell culture media. The two side channels that allow diffusion perpendicular to the light gradient direction were used to minimize the interference with the effect of light intensity, while the remaining channels were plugged.

The device was then fastened to the microscope stage. The bright field light from a halogen lamp of the microscope was focused onto one array of microhabitats, and the room temperature was kept at 25°C during all the experiments. The other array microhabitat on the same membrane was exposed to no light and was used as a control. The no light condition was confirmed with a PAR meter.

Millimeter scale light gradient generation and 96 well plate setup

The light intensity gradient was generated by a 5 inch by 5 inch LED matrix with 32 x 32 individually addressable LED light (Adafruit 32x32 RGB LED Matrix - 4 mm pitch). To generate a light intensity gradient, the LED matrix was programmed to be half on and half off using an Arduino micro-controller. A gap of 5 cm was designed in the fixture between the plate and the LED matrix, where air flow was created by four fans (Comidox Black brushless DC cooling Blower fan 5015S 5V) on the two sides to ensure uniform temperature in the system.

The light intensity gradient was quantified using the PAR (Photosynthetically Active Radiation) meter (Apogee MQ-501) placed on the bottom plane of the 96-well plate. By measuring the light intensity at each well position on the 96-well plate, a well-defined light gradient generation was verified on a 6-row × 9-column well area.

Sterile plastic 96 well plates (Flat bottom, Polystyrene, Falcon, Corning) were used for experiments using *M. aeruginosa* or *C. reinhardtii* and LED light matrix. 150uL of cell culture was introduced into each well. A plate sealing film (AeraSeal film, BS-25, Sigma-Aldrich) was applied tightly on top of the well, together with a plate cover to ensure sterility. The sealing film was found to be essential to avoid evaporation. The whole system was kept in a temperature-controlled incubator (e. g. 31°C) (Imperial III, Lab-line) for 9 days for *M. aeruginosa* and around 3 days for *C. reinhardtii*.

Imaging and data analysis

Imaging and data analysis for microhabitat experiment. The number of *C. reinhardtii* cells in the microhabitats was quantified using the autofluorescence of the chlorophyll from the cells and a fluorescence microscope (Olympus IX81, Center Valley, CA). Excitation light was generated by a fluorescence lamp (X-Cite 120PC Q, Excelitas Technologies Corp.), together with a 488/10 nm single bandpass excitation filter (Semrock, Rochester, NY). Emission light was collected by an EMCCD camera (ImagEM X2 EM-CCD camera, Hamamatsu Photonics K.K.) along with a 440/521/607/700 quad-bandpass emission filter (Semrock, Rochester, NY). Fluorescence images were taken every 4 hours for 7 days with exposure time of 50 ms. ImageJ was used for data analysis, where cell number was treated as proportional to fluorescence intensity. This method was validated by cell counts in bright field images. The specific growth rates were obtained by fitting the exponential growth phase of each habitat's growth curve to a linear function.

Data collection and analysis for 96 well plate experiment. For experiments using 96 well plate, the plate was taken out of the incubator for cell density quantification every day for *M. aeruginosa* and about twice a day for *C. reinhardtii*, starting from the initiation of the cell culture. The cell density was measured using a plate reader (Biotek synergy 2 multi-mode plate reader) at 665 nm and 730 nm, using chlorophyll absorbance and culture turbidity, respectively. To calibrate the optical density readings from the plate reader to cell density, we counted cells under the microscope using a hemocytometer and identified linear relationships of optical density and cell density at both wavelengths.

Cell culture and media

Chlamydomonas reinhardtii. *C. reinhardtii* wild type strain CC-125 was obtained from the Stern Laboratory at the Boyce Thompson Institute of Plant Research on the Cornell University campus. Cells were maintained in minimal medium (MM) with 10% Tris Acetate Phosphate (TAP) medium (2mM Tris, 1.7mM Acetate, 0.68 mM K_2HPO_4, 0.45mM KH_2PO_4, 7.5 mM NH_4Cl, and other salts including 0.34 mM $CaCl_2$) prepared using an established

protocol[37] with trace metal elements concentrations as described in Hutner et al[38]. 5mL cell culture was maintained in 15mL glass tubes in a temperature-controlled incubator at 25°C without shaking (New Brunswick Innova 44, Eppendorf) under an illumination of 12 µmol·m^{-2}·s^{-1} using LED light (4000K, Commercial Electric).

To set up the light intensity gradient experiment, cells from exponential growth phase were used (typically day 2 after transferring a culture). Cell cultures were concentrated to around 7.6 × 10^5 cells/mL before cell seeding to the microhabitat. Cell cultures were diluted to around 5 × 10^4 cells/mL to initiate the 96 well plate experiment.

***Microcystis aeruginosa*.** *M. aeruginosa PCC 7806* strain was purchased from the Pasteur Culture Collection of Cyanobacteria, Institut Pasteur, Paris, France. *M. aeruginosa PCC 7806* was routinely cultured in BG11 media (17.6 mM of $NaNO_3$, 0.22 mM K_2HPO_4, 0.3 mM $MgSO_4·7H_2O$, 0.2 mM $CaCl_2·2H_2O$, 0.03 mM Citric Acid ·H_2O, 0.02 mM Ferric Ammonium Citrate, 0.002 mM $Na_2EDTA·2H_2O$, 0.18 mM Na_3CO_3) (UTEX Culture Collection of Algae)**Error! Reference source not found.**. The regular cultures were incubated in 15 mL glass culture tubes at 25°C without shaking under illumination of 12 µmol·m^{-2}·s^{-1}. Cell cultures for the light intensity gradient were harvested at early-exponential growth phase, or 3 to 4 days after transfer. Cell cultures were diluted to around 2.5 × 10^6 cells/mL to initiate the 96 well plate experiment.

Results and Discussion

Development of a micro-scale light intensity gradient via the modification of a commercial microscope

We took advantage of the two separate light paths in a commercially available epi-fluorescence microscope, Olympus IX 81. We modified the bright field light path to provide a light intensity gradient and utilized the epi-fluorescence light path for imaging the PSMs. More specifically, the light intensity gradient was generated by placing a half-moon patterned mask directly below the field iris along the transmitted light path of the microscope (Fig. 1A). The light from the halogen lamp of the microscope passed through the collector lens, half-moon mask, field/condenser lens, and formed an inverted light intensity pattern in the sample plane. The position of the mask was secured by a 3D-printed plastic frame, as the light-dark transition region was sensitive to the movement of the mask. Fig. 1B is a bright field image of the light intensity gradient imaged by the CCD camera, with the array microhabitat in focus in the sample plane.

The micrometer-scale light intensity gradient was characterized using a CCD camera and a PAR meter. Bright field images were taken by the camera at the imaging plane and PAR values were

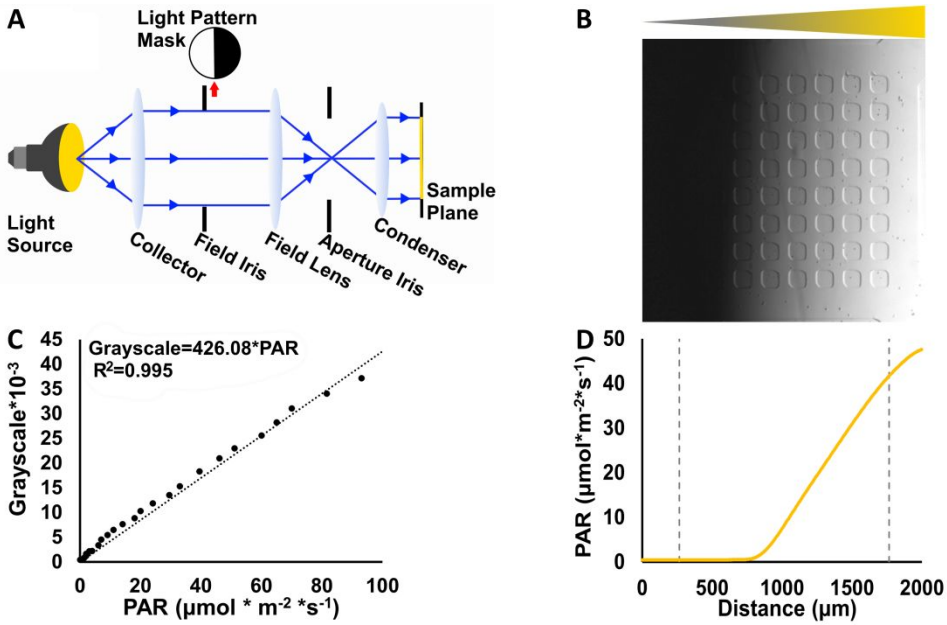

Figure 1. Experimental setup for micrometer-scale light intensity gradient generation and characterization. (A) Modifying the bright field light path of an Olympus IX 81 for light gradient generation (Note: not all the light rays are drawn). Light comes from a halogen lamp. A half-moon light pattern mask was placed directly below the field iris to create the light gradient. Both field and aperture irises were fully open throughout all experiments for optimal, reproducible light gradient generation. A wide field iris allows a large illumination area on the sample plane, while a wide aperture collects multiple illumination angle sources, as explained by Kohler illumination. **(B)** A bright field image of an array microhabitat illuminated by the light gradient generator. The image is 2.048mm x 2.048mm size. Each array microhabitat contains 8 x 8 habitats, and each habitat has the size of 100 µm × 100 µm × 100 µm. **(C)** Calibration curve of grayscale value from the CCD camera as a function of the light intensity measured by the PAR (photosynthetic active radiation) meter. Dots are the adjusted grayscale values, and the line is a fit to a linear function. **(D)** The light intensity gradient profile. The PAR values along the y-axis were obtained from converting images taken by the CCD camera to PAR value using the fitted equation in (C).

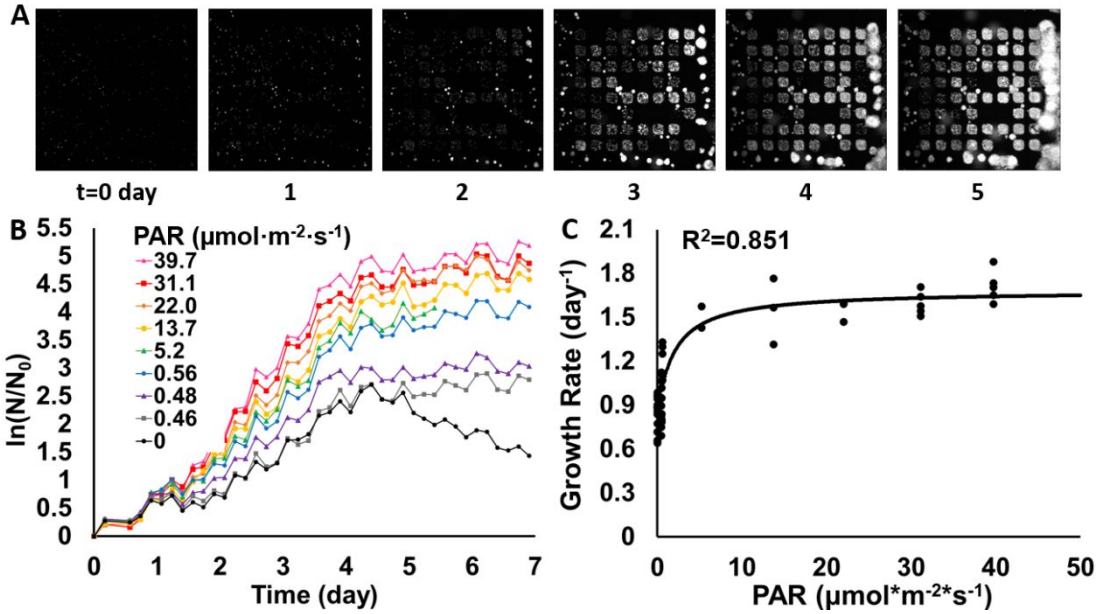

Figure 2. Growth response of *C. reinhardtii* to light intensity gradient in an array microhabitat. (A) A time series (5 days) of fluorescence images of *C. reinhardtii* cells growing in an 8 × 8 array of microhabitats under a light intensity gradient, with approximately 0 PAR on the left side and about 47.7 PAR on the right. Each microhabitat is 100 μm × 100 μm × 100 μm. The size of each image is 2.048 mm × 2.048 mm. **(B)** Growth curves of *C. reinhardtii* cells at various light intensities. Each curve is an average of growth curves of at least 3 habitats per the same column. PAR values represent light intensity at each column of habitats, with 0 PAR representing the control habitats. **(C)** Growth rate of *C. reinhardtii* cells as a function of PAR. Dots are experimental values and line is a fit to Monod model (Equation 1). The fitted coefficients with 95% confidence bounds are μ_0=0.823±0.07 day^{-1} μ_{max}'=0.860±0.099 day^{-1}, and K_S=1.9±1.18 μmol/(m²∗s), with an R-squared value of 0.851. This data is collected from 1 of 3 replicates.

taken at the location of the sample plane at various lamp light intensities. The adjusted grayscale values from the camera are shown to be linearly related to the PAR values (0 to 102 μmol·m^{-2}·s^{-1} PAR) (Fig. 1C). We note that the camera is very sensitive to light, thus neutral density filters and exposure time were used to keep the light intensity within the camera's dynamic range. In the following experiments, all light intensity values (grayscale) were recorded using the camera, and the formula in Fig. 1C was used to convert the adjusted grayscale to the PAR value. Fig. 1D shows the light intensity gradient across the array microhabitat (Fig. 1B).

The presented micrometer-scale light intensity gradient generation system can be easily adapted to various other studies involving PSMs. This system can be used with a variety of microfluidic chips and other devices, as long as they fit on a microscope stage. The characteristics of the light gradient can be easily modified via lamp voltage, optical mask, or other settings to quantify additional light sensitive behaviours, such as phototaxis. The light gradient generation can also be used in conjunction with gradients of other environmental conditions including nutrient concentration or temperature gradients to recreate a natural complex environment [39-41].

The impact of light intensity gradient on the growth of *C. reinhardtii* using an array microhabitat

Quantitative growth response of *C. reinhardtii* cells to light intensity was explored using the light intensity gradient generated in Fig. 1 together with a previously-developed array microhabitat device [39] (Fig. 2). For a typical experiment, the array microhabitats were first seeded with algal cells, at an initial seeding density of several cells per habitat. The array microhabitats containing cells were then placed on the microscope stage under the light intensity gradient. Fluorescence images were taken every 4 hours for about 7 days on the same microscope stage.

The time series images are shown in Fig. 2A. A roughly uniform seeding was observed at day 0. Difference in cell growth between the lighter and the darker side of the array began to emerge at day 2 and the contrast continued to increase until day 5. Here, the chlorophyll fluorescence (488 nm/700 nm, ex/em) was used as a measure of cell number (N). Growth curves for each column corresponding to various light intensities were calculated via ln(N)/ln(N_0) and plotted in Fig. 2B, with N_0 being the initial fluorescence intensity in a habitat. It is clear from Fig. 2B that cells' growth rate increases with the light intensity. The cell growth reaches a plateau at about 4-5 days at all light intensities. Note, we see that cell number decreased after day 5 at 0 μmol·m^{-2}·s^{-1}, possibly due to cell death after that point. Growth rates under different light intensities were calculated by fitting the exponential region (from about day 2-4) of an individual habitats' growth curve to a linear function. The growth rate, or the fitted slope, was then plotted as a function of PAR value (Fig. 2C). The data shown in Fig. 2 is from one of the three repeated experiments.

We note that the initial cell number within each habitat varied from about 0 to 8 cells. This leads to a few dark habitats at a later stage in Fig. 2A. In addition, there were cells outside the

habitats during seeding, and occasionally, these cells grew into the habitats. In our data analysis, we excluded data from habitats in which the initial cell number is zero or cells grew into the habitats at a later stage from surrounding area. In a previous study from our lab, initial number of cells was not found to affect the growth rate obtained at exponential growth phase [42].

The Monod growth kinetics model was used to fit the curve of growth rate versus PAR. Here, we use light intensity as a sole control parameter, as we hypothesize that light intensity would be the limiting substrate for the algal growth in our system. The Monod model has been widely used for microalgae growth and can describe the growth saturation behavior [43], it is described as follows:

$$\mu = \mu_0 + (\mu_{max}' * S)/(K_S + S). \quad (1)$$

Here, μ_0 is the initial growth rate, μ_{max}' is the maximum specific growth rate without baseline growth, S is the light intensity, and K_S is the half-saturation constant with respect to light intensity [43]. We note that μ_0 was included in the model because there was a baseline growth at the 0 PAR light condition, as the culture medium contained acetate as a carbon and energy source which allowed PSM growth in the dark. Fitting equation 1 to our data (Fig. 2C), we found μ_0 =0.823 day^{-1}, μ_{max}' =0.860 day^{-1}, K_S =1.9 µmol·m^{-2}·s^{-1}, and the maximum specific growth rate $\mu_{max} = \mu_0 + \mu_{max}'$ =1.68 day^{-1}.

Previously, K_S was reported to be 81.4 to 215 µmol·m^{-2}·s^{-1} for *C. reinhardtii* grown in a macro-scale photobioreactor and fit to a Monod model [44]. The low K_S value (1.9 µmol·m^{-2}·s^{-1}) obtained in this experiment shows *C. reinhardtii* cells on a microfluidic platform are more sensitive to light intensity than cells in large scale experiments. This difference could be due to (1) the self-shading that is common in large scale culture, and/or (2) the different light spectrum of the light source. The maximum growth rate μ_{max} (1.68 day^{-1}) obtained in this experiment was in the lower end of the range (1.4 to 5.46 day^{-1}) reported for *C. reinhardtii* grown in a macro-scale photobioreactor and fit to a Monod model [43].

The van Oorschot (Poisson) model has also been used in multiple previous studies to describe microalgal growth [44-46]. The van Oorschot model [43] uses the same parameters as the Monod model and is described as follows:

$$\mu = \mu_0 + \mu_{max}' * (1 - e^{-S/K_S}). \quad (2)$$

Fitting equation 2 to our data (Fig. S2), we found μ_0 = 0.826 day^{-1}, μ_{max}'= 0.787 day^{-1}, K_S = 2.03 µmol·m^{-2}·s^{-1} and $\mu_{max} = \mu_0 + \mu_{max}'$ =1.61 day^{-1}. Our experimental μ_{max} was found to be consistent with values previously reported in the literature for other microalgal species grown in photobioreactors and fit to the van Oorschot model, while our K_S value was typically several orders of magnitude lower than literature values.[43]. Here, values from the Monod model and van Oorschot are consistent, with both models fitting the data equally well based on R-squared value (Fig. 2C and S2).

Development of a millimeter-scale light intensity gradient via programming an individually addressable LED matrix

A light intensity gradient was successfully generated at the bottom of a 96 well plate (Fig. 3A) using an LED matrix. A 96 well plate is a common platform for cell culture, and especially suitable for *M. aeruginosa* due to its slow growth rate. A 3D printed fixture was used to align the LED matrix and the 96 well plate (Fig. 3B). The color spectrum of the light source was defined in the program as equal contribution of R, G, B for white light, and can be easily modified according to application. We note that fans were used to dissipate the heat generated by the LED matrix to maintain uniform temperatures across the 96 well plate area (Fig. S3).

The light intensity was measured using a PAR meter placed at the location of each well and was rendered in color in Fig. 3C. Since there is light shading along the edge of the 96 well plate, we used the middle portion of the 96 well plates (box in Fig. 3A) for experimental observation. Inside this area, the light intensities across the 4 rows (row C to row F) were uniform and were measured to be 3-23 µmol·m^{-2}·s^{-1} across columns 3 through 11 (Fig. 3C). Fig. 3D shows a photo of *M. aeruginosa* cells growing in a 96 well plate under the light gradient at day 4. As the light intensity increased from left to right, wells became a darker green, which indicated that *M. aeruginosa* grew faster under higher light intensity.

This light intensity gradient generation system using a 96 well plate could be easily adapted in bioscience labs to study photosynthetic micro- and macro-organisms. Specifically, the system could be used in fast screening of light intensity

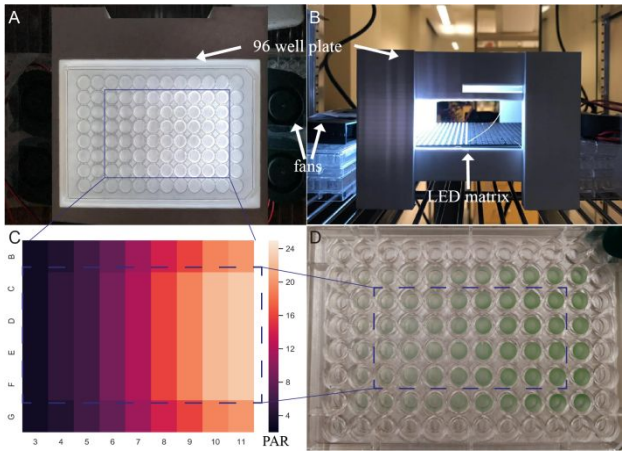

Figure 3. The light intensity generator for a 96 well plate. (A&B) The top(A) and front(B) view of the experimental setup. The overall experimental setup was a 3D printed structure that has two stacked platforms. The top platform holds the 96 well plate and the bottom platform holds the computer-controlled LED matrix. The distance between the platforms is 4cm. Each LED in the LED matrix was controlled individually using an Arduino board. To prevent the temperature gradient caused by the LED matrix, four fans (black) were placed along the sides of the device, providing air flow between the two platforms. **(C)** The PAR value (µmol·m^{-2}·s^{-1}) at the location of the 96 well plate. The color was rendered using the measured PAR value. The light intensity ranged from 3 to 23 µmol·m^{-2}·s^{-1}. **(D)** An image of the 96 well plate seeded with the *M. aeruginosa* taken at day 4. Only the middle portion of the wells was used due to light shading at the outer edge.

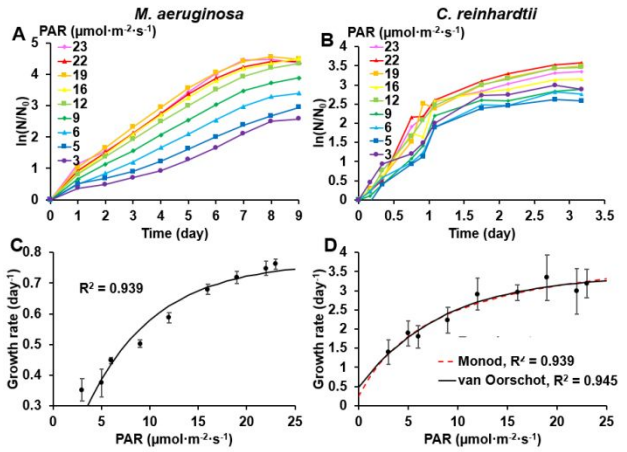

Figure 4. Light intensity regulates the growth rate of *M. aeruginosa* and *C. reinhardtii* in a 96-well plate. (A, B) The growth curves of *M. aeruginosa* **(A)** and *C. reinhardtii* **(B)** under various light intensities at temperature 31°C. Average cell number (N) was obtained by measuring absorbance at 665 nm using a plate reader and averaging from results of replicated wells at the same light intensity. **(C, D)** The growth rates of *M. aeruginosa* **(C)** and *C. reinhardtii* **(D)** under different light intensities at temperature 31°C. The growth rates were calculated using the growth curves of individual wells, and the error bars represent standard error of the mean (SEM). For *M. aeruginosa* **(C)**, the fitted van Oorschot (Equation 2) coefficients with 95% confidence bounds are μ_{max}=0.77±0.08 day^{-1}, and K_S=7.17±2.19 μmol·m^{-2}·s^{-1}, with an R-square value of 0.939. For *C. reinhardtii* **(D)**, the fitted Monod (Equation 1) coefficients with 95% confidence bounds are μ_0=0.253±2.11 day^{-1}, μ_{max}'=4.03±1.10 day^{-1}, and K_S=7.97±16.1 μmol·m^{-2}·s^{-1}, with an R-square value of 0.939; the fitted van Oorschot (Equation 2) coefficients with 95% confidence bounds are μ_0=0.473±1.16 day^{-1}, μ_{max}'=2.93±0.815 day^{-1}, and K_S=8.41±7.69 μmol·m^{-2}·s^{-1}, with an R-square value of 0.945. The Monod fit is shown in red dashed line and van Oorschot in black solid line.

conditions in culturing other cyanobacteria and microalgae. It could also be applied in the study of plant sprout development in response to light [47, 48]. In addition, the light spectrum is not limited within the visible light range due to available ultra-violet and infra-red LEDs, which allow further applications in biology and beyond.

The impact of light intensity on the growth of PSMs using a 96 well plate

Using the millimeter scale light intensity gradient system in Fig. 3, we quantified the growth response of monocultures of *M. aeruginosa* (Figure 4A, C) and *C. reinhardtii* (Fig. 4B, D) to light intensity gradients using a 96 well plate. The average growth curves of *M. aeruginosa* under different light intensities are shown in Fig. 4A, which shows that cell growth increases with the PAR value (Fig. 4C). The growth rate dramatically increased when the light intensity was near 9 μmol·m^{-2}·s^{-1} and gradually approached saturation at higher light intensities.

Van Oorschot growth kinetics model (Equation 2) was used to fit the growth data (Fig. 4C). We note that this model has been used to model the growth response of *Microcystis* to light [49] and provided a better fit for our data than Monod kinetics model. Here, we chose μ_0 equals 0, and thus $\mu_{max} = \mu_{max}'$ in our fitting, because the cells were under photoautotrophic growth condition and thus no growth was expected at 0 μmol·m^{-2}·s^{-1}. The fitted results provided the maximum growth rate (μ_{max}) to be 0.77 day^{-1} and the half-saturation constant (K_S) to be 7.17 μmol·m^{-2}·s^{-1}. Our work is consistent with previous work using *M. aeruginosa* in a flask setting, which provided K_S of 8.79±0.63 μmol·m^{-2}·s^{-1} and μ_{max} of 0.211±0.006 day^{-1} at 20 °C [49]. Using the 96 well plate setup at 25°C (Fig. S4), we found the μ_{max} to be 0.57±0.27 day^{-1} and the K_S to be 10.41±10.23 μmol·m^{-2}·s^{-1}. We note that at the lower temperature, *M. aeruginosa* grows more slowly, leading to poor fitting of the kinetic model. Further screening on temperature could help elucidate the interplay of temperature and light on the growth of the cyanobacteria.

The growth of the model algal *C. reinhardtii* was also studied in the 96-well plate setup (Fig. 4B). The growth rate of *C. reinhardtii* versus light intensity was fitted to the Monod kinetics (Equation 1) model (Fig. 4D), and the results showed that μ_0=0.253 day^{-1}, μ_{max}'=4.03 day^{-1}, K_S=7.97 μmol·m^{-2}·s^{-1}, and μ_{max} =4.283 day^{-1} (R-square 0.939), while fitting the van Oorschot kinetics (Equation 2) gave the coefficients of μ_0=0.473 day^{-1}, μ_{max}'=2.93 day^{-1}, K_S=8.41 μmol·m^{-2}·s^{-1}, and μ_{max} = 3.403 day^{-1} (R-square 0.945). The fitted maximum specific growth rates are within the range reported in the literature (1.4 day^{-1} to 5.46 day^{-1} [43]).

To summarize, Fig. 4 shows that *C. reinhardtii* and *M. aeruginosa* have similar half-saturation constant K_S, which means that their response sensitivity to light intensity is comparable. Despite similar sensitivity to light, the μ_{max} of *C. reinhardtii* tells us that it has much higher growth rate, or a 5-fold increase, than that of *M. aeruginosa*. At the moment, to grow *M. aeruginosa* in the microfluidic platform is still a challenge, possibly due to its slow growth rate.

Conclusions and future perspectives

In this paper, we developed a microscope-based light gradient generation system for high throughput and quantitative study of photosynthetic microorganisms. Using this system, we quantified the growth of a model alga *C. reinhardtii* in response to light intensity in an array of microhabitats. For comparison, we also studied the growth response to light intensity of *C. reinhardtii* and *M. aeruginosa* in a 96 well plate set up.

Our experimental results showed that the growth of *C. reinhardtii* and *M. aeruginosa* under light intensity gradients followed a Monod/van Oorschot kinetic model in all cases. Interestingly, the growth sensitivity to light, measured by the kinetic constant K_S in the same 96-well plate set up, is similar for the alga *C. reinhardtii* and cyanobacteria *M. aeruginosa* under the same temperature (Table S1). This could indicate some generality in PSMs' utilization of light but needs to be verified by experiments using a larger range of light intensities and other PSMs. In parallel to this, the maximum growth rate is 5.5-fold higher for *C. reinhardtii* than that of *M. aeruginosa*. A second interesting finding is that the measured K_S was significantly smaller using the microfluidic device than that from the large-scale device (Table S1). For *C. reinhardtii*, it is 1.9 μmol·m^{-2}·s^{-1} using our microfluidic platform (halogen light at 25

°C), 7.97 μmol·m^{-2}·s^{-1} (LED array, 31 °C) using 96 well plate assay, and 81.4 to 215 μmol·m^{-2}·s^{-1} using a large-scale bioreactor (various light sources and temperature, some not reported), from existing literature (See table in supplementary materials for details). One possible explanation is self-shading of the cells that reduce the efficiency of utilization of incident light in large containers as compared to the microhabitats. A second important factor is the spectrum of the light sources. The halogen lamp from the microscope has a continuous emission spectrum across 400-700nm, whereas RGB LEDs from the 96 well plate assay have three discrete peaks between with 10-30nm bandwidth [50]. Light with different wavelength differentially affect the absorption of photosynthetic pigments in PSMs and can regulate their metabolism. A last explanation can be temperature. While the kinetic constants obtained here can be used to guide the future design of large-scale bioreactors for the production of biofuels or ecological studies, one must keep in mind that the size of the device, the temperature, the light spectrum, as well as cycles of light are all important for the growth of PSMs.

Looking forward, we expect the presented technology will find wide applications in understanding the impact of environmental parameters on the PSMs' growth for maintaining the balance of aquatic ecosystems, as well as finding alternative bioenergy solutions. One example is to use this technology to screen light and chemical/nutrient condition to optimize the production of biolipids for biofuel production. Here, the microscope-based light gradient platform along with the gradient generation microfluidic chip can be used to generate well defined light intensity and nutrient conditions for the PSMs in a high throughput way. To detect the lipid content of the PSMs, one can either perfuse fluorescent dyes (Nile red, BODIPY) through the side channels to stain cells to reveal the cellular lipid content [51-55], or use optical-based label-free methods such as Raman spectroscopy for quantifying the biolipid content of lipid-producing microalgae [56-60].

Author Contributions

FL, LG, and MW created and designed the research project. LG and FL carried out the micro-scale experiments, FS, DV, and FL carried out the millimeter scale experiments. LG and FL performed data analysis. All authors participated in the writing and discussion of the manuscript.

Conflicts of interest

There are no conflicts to declare.

Acknowledgements

This work is supported by the USDA National Institute of Food and Agriculture, AFRI project [2016-08830], the Academic Venture Fund from the Cornell Atkinson Center for Sustainability, and The New York State Hatch fund. This work was performed in part at the Cornell NanoScale Facility, a member of the National Nanotechnology Coordinated Infrastructure (NNCI), which is supported by the National Science Foundation (Grant NNCI-2025233). We thank the capstone project team from the Bioinstrumentation course at Cornell (student: SoYoung Min and Monica Young, TA: Brain Cheung and Ehsan Esmaili, Instructor: Dr. Sunghwan Jung) for building the prototype for the macro-scale light intensity platform. We thank Prof. Ahner, Prof. Winans and Dr. Mohammad Yazdani for insightful discussions.

Notes and references

1. J. Xiong, W. M. Fischer, K. Inoue, M. Nakahara and C. E. Bauer, *Science*, 2000, **289**, 1724-1730.
2. R. E. Blankenship, *Science*, 2017, **355**, 1372-1373.
3. C. J. Gobler, *Harmful Algae*, 2020, **91**, 101731.
4. H. W. Paerl and M. A. Barnard, *Harmful Algae*, 2020, **96**, 101845.
5. S. B. Watson, C. Miller, G. Arhonditsis, G. L. Boyer, W. Carmichael, M. N. Charlton, R. Confesor, D. C. Depew, T. O. Hook, S. A. Ludsin, G. Matisoff, S. P. McElmurry, M. W. Murray, R. P. Richards, Y. R. Rao, M. M. Steffen and S. W. Wilhelm, *Harmful Algae*, 2016, **56**, 44-66.
6. H. Xu, H. W. Paerl, G. W. Zhu, B. Q. Qin, N. S. Hall and M. Y. Zhu, *Hydrobiologia*, 2017, **787**, 229-242.
7. M. A. Chia, J. G. Jankowiak, B. J. Kramer, J. A. Goleski, I. S. Huang, P. V. Zimba, M. do Carmo Bittencourt-Oliveira and C. J. Gobler, *Harmful Algae*, 2018, **74**, 67-77.
8. T. W. Davis, D. L. Berry, G. L. Boyer and C. J. Gobler, *Harmful Algae*, 2009, **8**, 715-725.
9. J. Leon-Munoz, M. A. Urbina, R. Garreaud and J. L. Iriarte, *Sci Rep-Uk*, 2018, **8**.
10. M. Á. Lezcano, A. Quesada and R. El-Shehawy, *Harmful Algae*, 2018, **71**, 19-28.
11. M. Z. Liu, J. R. Ma, L. Kang, Y. Y. Wei, Q. He, X. B. Hu and H. Li, *Sci Total Environ*, 2019, **670**, 613-622.
12. S. Sliwinska-Wilczewska, A. Cieszynska, M. Konik, J. Maculewicz and A. Latala, *Estuar Coast Shelf S*, 2019, **219**, 139-150.
13. W. E. A. Kardinaal, L. Tonk, I. Janse, S. Hol, P. Slot, J. Huisman and P. M. Visser, *Appl Environ Microb*, 2007, **73**, 2939-2946.
14. C. P. Deblois and P. Juneau, *J Phycol*, 2012, **48**, 1002-1011.
15. S. L. Renaud, F. R. Pick and N. Fortin, *Appl Environ Microb*, 2011, **77**, 7016-7022.
16. M. Roy and K. Mohanty, *Algal Res*, 2019, **44**.
17. J. R. Ziolkowska, *Biofuels for a More Sustainable Future: Life Cycle Sustainability Assessment and Multi-Criteria Decision Making*, 2020, DOI: 10.1016/B978-0-12-815581-3.00001-4, 1-19.
18. P. Pal, K. W. Chew, H. W. Yen, J. W. Lim, M. K. Lam and P. L. Show, *Sustainability-Basel*, 2019, **11**.
19. C. S. Jones and S. P. Mayfieldt, *Curr Opin Biotech*, 2012, **23**, 346-351.
20. M. A. Borowitzka, *J Appl Phycol*, 2013, **25**, 743-756.
21. Q. Jiang, X. R. Song, J. Liu, Y. Q. Shao and Y. J. Feng, *Water Res*, 2019, **167**.
22. S. Mishra and K. Mohanty, *Bioresource Technol*, 2019, **273**, 177-184.

23. S. N. Mohamed, P. A. Hiraman, K. Muthukumar and T. Jayabalan, *Bioresource Technol*, 2020, **295**.
24. C. N. Reddy, H. T. H. Nguyen, M. T. Noori and B. Min, *Bioresource Technol*, 2019, **292**.
25. W. Zevenboom and L. R. Mur, *Arch Microbiol*, 1984, **139**, 232-239.
26. E. Banares-Espana, J. C. Kromkamp, V. Lopez-Rodas, E. Costas and A. Flores-Moya, *Fems Microbiol Ecol*, 2013, **83**, 700-710.
27. M. Xiao, A. Willis and M. A. Burford, *Harmful Algae*, 2017, **62**, 84-93.
28. F. Liu, A. Giometto and M. Wu, *Anal Bioanal Chem*, 2021, **413**, 2331-2344.
29. P. J. Graham, J. Riordon and D. Sinton, *Lab Chip*, 2015, **15**, 3116-3124.
30. S. K. Choudhary, A. Baskaran and P. Sharma, *Biophys J*, 2019, **117**, 1508-1513.
31. J. Arrieta, A. Barreira, M. Chioccioli, M. Polin and I. Tuval, *Sci Rep-Uk*, 2017, **7**.
32. J. Arrieta, M. Polin, R. Saleta-Piersanti and I. Tuval, *Phys Rev Lett*, 2019, **123**.
33. C. T. Kreis, M. Le Blay, C. Linne, M. M. Makowski and O. Baumchen, *Nat Phys*, 2018, **14**, 45-49.
34. Y. J. Sung, H. S. Kwak, M. E. Hong, H. I. Choi and S. J. Sim, *Anal Chem*, 2018, **90**, 14029-14038.
35. A. T. Lam, K. G. Samuel-Gama, J. Griffin, M. Loeun, L. C. Gerber, Z. Hossain, N. J. Cira, S. A. Lee and I. H. Riedel-Kruse, *Lab Chip*, 2017, **17**, 1442-1451.
36. H. S. Kim, T. L. Weiss, H. R. Thapa, T. P. Devarenne and A. Han, *Lab Chip*, 2014, **14**, 1415-1425.
37. R. K. Togasaki, K. Brunke, M. Kitayama and O. M. Griffith, in *Progress in Photosynthesis Research: Volume 3 Proceedings of the VIIth International Congress on Photosynthesis Providence, Rhode Island, USA, August 10–15, 1986*, ed. J. Biggins, Springer Netherlands, Dordrecht, 1987, DOI: 10.1007/978-94-017-0516-5_106, pp. 499-502.
38. S. H. Hutner, *J Bacteriol*, 1946, **52**, 213-221.
39. F. Liu, M. Yazdani, B. A. Ahner and M. Wu, *Lab Chip*, 2020, **20**, 798-805.
40. W. Wang, L. Li, M. Ding, G. Luo and Q. Liang, *BioChip Journal*, 2018, **12**, 93-101.
41. J. Y. Zhu, S. A. Suarez, P. Thurgood, N. Nguyen, M. Mohammed, H. Abdelwahab, S. Needham, E. Pirogova, K. Ghorbani, S. Baratchi and K. Khoshmanesh, *Anal Chem*, 2019, **91**, 15784-15790.
42. B. J. Kim, L. V. Richter, N. Hatter, C. K. Tung, B. A. Ahner and M. M. Wu, *Lab Chip*, 2015, **15**, 3687-3694.
43. E. Lee, M. Jalalizadeh and Q. Zhang, *Algal Res*, 2015, **12**, 497-512.
44. P. Darvehei, P. A. Bahri and N. R. Moheimani, *Renewable and Sustainable Energy Reviews*, 2018, **97**, 233-258.
45. R. J. Geider, H. Maclntyre, T. M. J. L. Kana and Oceanography, 1998, **43**.
46. Q. Béchet, P. Chambonnière, A. Shilton, G. Guizard and B. Guieysse, 2015, **112**, 987-996.
47. M. Simlat, P. Ślęzak, M. Moś, M. Warchoł, E. Skrzypek and A. Ptak, *Scientia Horticulturae*, 2016, **211**, 295-304.
48. E. Reed, C. M. Ferreira, R. Bell, E. W. Brown, J. Zheng and D. W. Schaffner, 2018, **84**, e02814-02817.
49. K. Hesse, E. Dittmann and T. Borner, *Fems Microbiol Ecol*, 2001, **37**, 39-43.
50. M. Glemser, M. Heining, J. Schmidt, A. Becker, D. Garbe, R. Buchholz and T. Brück, *Appl Microbiol Biot*, 2016, **100**, 1077-1088.
51. J. Rumin, H. Bonnefond, B. Saint-Jean, C. Rouxel, A. Sciandra, O. Bernard, J.-P. Cadoret and G. Bougaran, *Biotechnology for Biofuels*, 2015, **8**, 42.
52. R. E. Holcomb, L. J. Mason, K. F. Reardon, D. M. Cropek and C. S. Henry, *Analytical and Bioanalytical Chemistry*, 2011, **400**, 245-253.
53. H. S. Kim, A. R. Guzman, H. R. Thapa, T. P. Devarenne and A. Han, 2016, **113**, 1691-1701.
54. H. S. Kim, S.-C. Hsu, S.-I. Han, H. R. Thapa, A. R. Guzman, D. R. Browne, M. Tatli, T. P. Devarenne, D. B. Stern and A. Han, 2017, **1**, e00011.
55. S. Mishra, Y.-J. Liu, C.-S. Chen and D.-J. Yao, 2021, **14**, 1817.
56. O. Samek, P. Zemánek, A. Jonáš and H. H. Telle, *Laser Physics Letters*, 2011, **8**, 701-709.
57. T. Wang, Y. Ji, Y. Wang, J. Jia, J. Li, S. Huang, D. Han, Q. Hu, W. E. Huang and J. Xu, *Biotechnology for Biofuels*, 2014, **7**, 58.
58. D. McIlvenna, W. E. Huang, P. Davison, A. Glidle, J. Cooper and H. Yin, *Lab Chip*, 2016, **16**, 1420-1429.
59. H. S. Kim, S. C. Waqued, D. T. Nodurft, T. P. Devarenne, V. V. Yakovlev and A. Han, *Analyst*, 2017, **142**, 1054-1060.
60. X. Wang, L. Ren, Y. Su, Y. Ji, Y. Liu, C. Li, X. Li, Y. Zhang, W. Wang, Q. Hu, D. Han, J. Xu and B. Ma, *Anal Chem*, 2017, **89**, 12569-12577.